

Proton-Coupled Electron-Transfer Reactions in $[\text{Mn}^{\text{IV}}_2(\mu\text{-O})_3\text{L}'_2]^{2+}$ ($\text{L}' = 1,4,7\text{-Trimethyl-1,4,7-triazacyclononane}$)

Ronald Hage,* Bert Krijnen, and Johann B. Warnaar

Unilever Research Laboratorium, Olivier van Noortlaan 120, 3133 AT Vlaardingen, The Netherlands

Frantisek Hartl, Derk J. Stufkens, and Theo L. Snoeck

Anorganisch Chemisch Laboratorium, Universiteit van Amsterdam, Nieuwe Achtergracht 166, 1018 WV Amsterdam, The Netherlands

Received October 20, 1994[®]

The $\text{p}K_{\text{a}}$ value of $[\text{Mn}^{\text{IV}}_2(\mu\text{-O})_3\text{L}'_2]^{2+}$ ($\text{L}' = 1,4,7\text{-trimethyl-1,4,7-triazacyclononane}$) has been determined spectrophotometrically by carrying out titration experiments with concentrated sulfuric acid. The extremely low $\text{p}K_{\text{a}}$ value of -2.0 suggests that the electron density on the bridging oxygen atoms is very small. The asymmetric Mn–O–Mn vibration is observed at 670 cm^{-1} , while the symmetric Mn–O–Mn vibration is present at 702 cm^{-1} . The unusually high frequencies of these vibrations are due to the small Mn–O–Mn angle of 78° . Protonation of an oxygen bridge shifts both the asymmetric and symmetric vibrations to 683 cm^{-1} . Electrochemical experiments in acetonitrile have shown that one-electron reduction of the complex is chemically irreversible. IR, EPR, and UV–vis studies of the reduced species suggest the presence of a $\text{Mn}^{\text{III}}\text{Mn}^{\text{IV}}(\mu\text{-O})_2(\mu\text{-OH})$ core. pH-dependent differential pulse voltammetry experiments in aqueous solutions have revealed an apparent $\text{p}K_{\text{a}}$ value of approximately 4.0 for the reduced mixed-valence species in various buffer systems. The reduction wave at $\text{pH} > 4$ is observed at around -0.10 V vs SCE . Cyclic voltammetry has revealed that the reduced species is prone to reaction with carboxylate groups. A bis(carboxylate)mono-oxo-bridged Mn(III)–Mn(III) species is formed in citric acid buffer which exhibits an anodic peak around $+0.6\text{ V vs SCE}$, and a UV–vis spectrum that is typical of such a species.

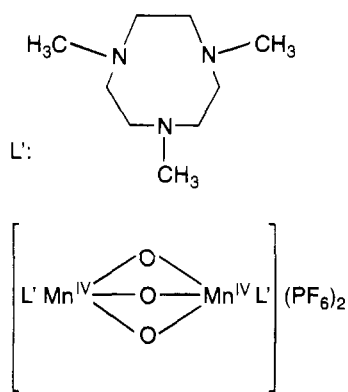
Oxidation of water in plants and algae occurs in photosystem II (PS II), which contains a tetranuclear manganese cluster.¹ During the oxidation, four electrons are generated and stored in this manganese cluster. A number of models have been put forward to explain the experimental data of this enzymatic system, including electron transfer reactions, proton transfer, and structural rearrangements.² Stabilization of the higher-valent manganese ions is thought to be caused by coupled electron–protonation processes. The higher-valent species can give rise to formation of an O–O bond out of two water molecules. Five distinct states of the complex have been identified; these have been denoted as the S states $\text{S}_0\text{--}\text{S}_4$.^{1–3} In one of the states of the cluster, the so-called S_2 state, a multiline EPR signal around $g = 2$ has been observed, indicative of a multinuclear mixed-valence species. Unfortunately, the exact structure of this cluster in any one of the states is not known presently. Mn–Mn distances of 2.7 and 3.3 Å have been inferred from X-ray absorption experiments on the active site of PS II.⁴

A number of model compounds have been reported which have two or more manganese ions in various oxidation states

and mimic some of the properties of the active site in PS II.⁵ An interesting class of dinuclear compounds has been reported by Wieghardt and co-workers. By using the capping tridentate ligands 1,4,7-triazacyclononane (L) and 1,4,7-trimethyl-1,4,7-triazacyclononane (L'), oxo-, hydroxo-, peroxy-, and acetato-bridged systems have been isolated and characterized.^{6–14} One of the complexes reported, $[\text{Mn}^{\text{IV}}_2(\mu\text{-O})_3\text{L}'_2]^{2+}$, exhibits rather unusual structural and physical properties¹² (see Chart 1).

- [®] Abstract published in *Advance ACS Abstracts*, September 1, 1995.
- (1) (a) Dismukes, G. C. *Photochem. Photobiol.* **1986**, *43*, 99. (b) George, G. N.; Prince R. C.; Cramer, S. P. *Science* **1989**, *243*, 789. (c) Renger, G. *Angew. Chem., Int. Ed. Engl.* **1987**, *26*, 643.
 - (2) Brudwig, G. W.; Thorp, H. H.; Crabtree, R. H. *Acc. Chem. Res.* **1991**, *24*, 311.
 - (3) McDermott, A. E.; Yachandra, V. K.; Guiles, R. D.; Cole, J. L.; Dexheimer, S. L.; Britt, R. D.; Sauer, K.; Klein, M. P. *Biochemistry* **1988**, *27*, 4021.
 - (4) (a) Rutherford, A. W.; Boussac, A.; Zimmermann, J.-L. *New J. Chem.* **1991**, *15*, 491. (b) Ono, T.-a.; Kusunoki, M.; Matsushita, T.; Oyanagi, H.; Inoue, Y. *Biochemistry* **1991**, *30*, 6836. (c) Wieghardt, K. *Angew. Chem., Int. Ed. Engl.* **1994**, *33*, 725.

- (5) (a) Wieghardt, K. *Angew. Chem., Int. Ed. Engl.* **1989**, *28*, 1153. (b) Christou, G. *Acc. Chem. Res.* **1989**, *22*, 328. (c) Brudwig, G. W.; Crabtree, R. H. *Prog. Inorg. Chem.* **1989**, *37*, 99. (d) Dismukes, C. G. In *Bioinorganic Catalysis*; Reedijk, J., Ed.; Marcel Dekker, Inc.: New York, 1993. (e) Thorp, H. H.; Brudwig, G. W. *New J. Chem.* **1991**, *15*, 479. (f) Que, L., Jr.; True, A. E. *Prog. Inorg. Chem.* **1990**, *38*, 97. (g) *Manganese Redox Enzymes*; Pecoraro, V. L., Ed.; VCH: New York, 1992. (h) Pecoraro, V. L.; Baldwin, M. J.; Gelasco, A. *Chem. Rev.* **1994**, *94*, 807.
- (6) Wieghardt, K.; Bossek, U.; Gebert, W. *Angew. Chem., Int. Ed. Engl.* **1983**, *22*, 328.
- (7) Wieghardt, K.; Bossek, U.; Ventur, D.; Weiss, J. *J. Chem. Soc., Chem. Commun.* **1985**, 347.
- (8) Wieghardt, K.; Bossek, U.; Bonvoisin, J.; Beauvillain, P.; Girerd, J. J.; Nuber, B.; Weiss, J.; Heinze, J. *Angew. Chem., Int. Ed. Engl.* **1986**, *25*, 1030.
- (9) Wieghardt, K.; Bossek, U.; Nuber, B.; Weiss, J. *Inorg. Chim. Acta* **1987**, *126*, 39.
- (10) Wieghardt, K.; Bossek, U.; Zsolani, L.; Huttner, G.; Blondin, G.; Girerd, J. J.; Babonneau, P. *J. Chem. Soc., Chem. Commun.* **1987**, 651.
- (11) Wieghardt, K.; Bossek, U.; Nuber, B.; Weiss, J.; Gehring, S.; Haase, W. *J. Chem. Soc., Chem. Commun.* **1988**, 1145.
- (12) Wieghardt, K.; Bossek, U.; Nuber, B.; Weiss, J.; Bonvoisin, J.; Corbella, M.; Vitols, S. E.; Girerd, J. J. *J. Am. Chem. Soc.* **1988**, *110*, 7398.
- (13) Bossek, U.; Weyermüller, T.; Wieghardt, K.; Nuber, B.; Weiss, J. *J. Am. Chem. Soc.* **1990**, *112*, 6387.
- (14) Niemann, A.; Bossek, U.; Wieghardt, K.; Butzlaff, C.; Trautwein, A. X.; Nuber, B. *Angew. Chem., Int. Ed. Engl.* **1992**, *31*, 311.

Chart 1. Schematic Representation of $[\text{Mn}^{\text{IV}}_2(\mu\text{-O})_3\text{L}'_2](\text{PF}_6)_2$ 

The Mn–Mn distance is only 2.296(2) Å, which is much shorter than that observed for other dinuclear Mn complexes. Typically, bis($\mu\text{-O}$)-bridged complexes show Mn–Mn distances of approximately 2.7 Å and the mono($\mu\text{-O}$)-bis($\mu\text{-carboxylate}$) complexes have an internuclear distance of 3.3 Å.⁵ Also the Mn–O–Mn angle of 78° is much smaller than usually observed. A consequence of this short Mn–Mn distance is the very strong coupling between the metal centers. Magnetic susceptibility measurements have revealed a coupling constant of -780 cm^{-1} , which is much larger than those found for any other dinuclear Mn system.¹² A good correlation has been observed between the M–M distance and coupling constant for dinuclear $\text{Mn}^{\text{IV}}\text{-Mn}^{\text{IV}}$ and $\text{Cr}^{\text{III}}\text{-Cr}^{\text{III}}$ complexes containing L' and various bridges, which has led to the conclusion that a direct M–M overlap is dominant in the metal–metal interaction in these systems.¹⁴

Because of these interesting properties, we decided to study some of the physical properties of this tris($\mu\text{-oxo}$)-bridged complex in greater detail. The pK_a value for the protonation of an oxygen bridge has been determined in order to obtain some information on the electronic properties of this molecule. The redox properties of this compound in CH_3CN and water at different pH values have been investigated as well. A number of model systems exhibit pH-dependent electrochemical potentials,^{15–18} and it will be shown that the tris($\mu\text{-O}$)-bridged dinuclear complex exhibits a very different behavior compared with that of other systems.

Experimental Section

Materials. All chemicals were used as obtained from the suppliers (Janssen Chimica and Aldrich). The ligand L' has been synthesized according to the procedure described before.¹⁹ $[\text{Mn}^{\text{IV}}_2(\mu\text{-O})_3\text{L}'_2](\text{PF}_6)_2\cdot\text{H}_2\text{O}$ (**1**) and $[\text{Mn}^{\text{III}}_2(\mu\text{-O})(\mu\text{-CH}_3\text{COO})_2\text{L}'_2](\text{PF}_6)_2$ (**2**) were prepared as described by Wieghardt and co-workers.¹² Elemental analyses of these compounds were in accordance with the literature values.

$[\text{Mn}^{\text{IV}}_2(\mu\text{-}^{18}\text{O})_3\text{L}'_2](\text{PF}_6)_2\cdot\text{H}_2\text{O}$ has been synthesized by the following method: A 1.20 g (1.36 mmol) sample of $[\text{Mn}^{\text{III}}_2(\mu\text{-O})(\mu\text{-CH}_3\text{COO})_2\text{L}'_2](\text{PF}_6)_2$ (**2**) was dissolved in acetonitrile (3 cm³), triethylamine (5 cm³), ethanol (3 cm³), and H_2^{18}O (2.5 cm³). Oxygen gas was passed through the solution for 5 h. After evaporation to dryness, the compound was recrystallized from ethanol. Yield: 780 mg (71%). Negative FAB-MS:²⁰ *m/s* 796 for $\{[\text{Mn}^{\text{IV}}_2(\mu\text{-}^{18}\text{O})_3\text{L}'_2](\text{PF}_6)_2\}^-$ and 790 for $\{[\text{Mn}^{\text{IV}}_2(\mu\text{-}^{16}\text{O})_3\text{L}'_2](\text{PF}_6)_2\}^-$.

Physical Measurements. UV–vis absorption measurements were performed on a HP 8452A spectrophotometer, using 1-cm quartz cells. pK_a titration experiments were carried out by adding concentrated sulfuric acid to an aqueous solution containing $[\text{Mn}^{\text{IV}}_2(\mu\text{-O})_3\text{L}'_2](\text{PF}_6)_2\cdot\text{H}_2\text{O}$ (**1**). The absorbances at 400, 440, 500, and 550 nm were measured at different acidity strengths, expressed as $-H_0$ values.²¹ Titration plots were made after correction for the dilution. The absorption bands (in nm) with extinction coefficients (in $\text{M}^{-1}\text{ cm}^{-1}$) in parentheses for **1** in water/sulfuric acid (50/50 v/v) are 300 (16×10^3), 432 (sh), 506 (0.8×10^3), 600 (sh), 752 (10), and 852 (13).

IR spectra were obtained on Bruker IFS 88 (KBr pellets) and BioRad FTS7 (spectroelectrochemistry) FTIR spectrometers. Resonance Raman spectra were recorded in KBr pellets on a Dilor XY Raman spectrometer. Excitation was performed at 458, 488, and 514.5 nm by using a SP Model 2016 argon ion laser.

Negative FAB-MS spectra were obtained on VG7070 and Trio-3 mass spectrometers by using nitrobenzyl alcohol as a matrix.²⁰

Differential pulse voltammograms (in aqueous and nonaqueous systems) and cyclic voltammograms (in aqueous solutions) were obtained on an EG&G PAR C Model 303 potentiostat with an EG&G PAR 384B polarograph analyzer and on an EG&G PAR Model 273A potentiostat. A glassy carbon electrode was used as working electrode, a saturated calomel electrode (SCE) as reference electrode, and a platinum wire as counter electrode. Before each experiment the glassy carbon electrode was polished with aluminum oxide. The scan rate for the cyclic voltammograms was 100 mV s^{-1} and for the differential pulse voltammograms was 4 mV s^{-1} . Cyclic voltammograms (nonaqueous systems) were realized on a PA4 (Ekomp, Czech Republic) potentiostat with a scan rate of $20\text{--}500\text{ mV s}^{-1}$. A Pt disk working electrode of 0.8 mm^2 area was used. The electrode was polished with a $1\text{ }\mu\text{m}$ diamond paste before the experiments. A silver wire was used as the pseudoreference electrode and a Pt gauze as the auxiliary electrode. For the bulk electrolysis experiments a platinum plate with a surface area of 2 cm^2 was used.

Tetrabutylammonium perchlorate (Bu_4NClO_4) (0.1 M) or tetrabutylammonium hexafluorophosphate (Bu_4NPF_6) (0.1 M) was used as supporting electrolyte in these solvents. Ferrocene was added to the solutions in acetonitrile as an internal standard for the determination of redox potentials and electrochemical reversibility of the redox steps.^{22a} Under the actual experimental conditions, E° of the ferrocene/ferrocenium couple (Fc/Fc^+) in CH_3CN was determined to be 0.39 V vs SCE . This agrees well with the value reported in the literature.^{22b} In acetonitrile containing 0.25 M sulfuric acid and 0.1 M Bu_4NClO_4 , the $E^\circ(\text{Fc}/\text{Fc}^+)$ potential is found to be 0.29 V vs SCE . In dmf the ferrocene/ferrocenium couple has a value of $E^\circ = 0.47\text{ V vs SCE}$. In CH_2Cl_2 the E° value of the ferrocene/ferrocenium couple reported is $+0.45\text{ V}$,^{22c} and in $\text{H}_2\text{O}/\text{Li}_2\text{SO}_4$ it is $+0.16\text{ V}$.^{22d} The UV–vis spectroelectrochemical experiments were performed on a Perkin Elmer Lambda 5 UV–vis spectrophotometer. An OTTLE cell²³ was used consisting of a Pt minigrad working electrode (32 wires/cm), a silver wire pseudoreference electrode, a Pt minigrad auxiliary electrode, and CaF_2 or quartz windows. The scan rate was 2 mV s^{-1} , and the supporting electrolyte was Bu_4NPF_6 (0.3 M). The concentration of the manganese compound was 10^{-2} M . The IR spectroelectrochemical experiments were carried out by using a BioRad FTS-7 FTIR spectrometer (16 scans, resolution 2 cm^{-1}) and the OTTLE cell as described above, but with NaCl windows. Citric and phosphoric acids (0.2 M) were the supporting electrolytes and buffers in the aqueous solutions. The concentration of L' in the ligand buffer was 0.1 M with 0.1 M NaClO_4 to obtain an ionic strength similar to that used for the phosphate and citrate buffer systems. The pH was adjusted by adding drops of 4 or 0.5 M NaOH or HCl and was measured in the cell, using a Schott Gerate CG 820 pH meter with an Ingold microelectrode.

(15) Manchanda, R.; Thorp, H. H.; Brudvig, G. W.; Crabtree, R. H. *Inorg. Chem.* **1991**, *30*, 494.

(16) Thorp, H. H.; Sarneski, J. E.; Brudwig, G. W.; Crabtree, R. H. *J. Am. Chem. Soc.* **1989**, *111*, 9249.

(17) Thorp, H. H.; Brudwig, G. W.; Bowden, E. F. *J. Electroanal. Chem. Interfacial Electrochem.* **1990**, *290*, 293.

(18) Manchanda, R.; Thorp, H. H.; Brudwig, G. W.; Crabtree, R. H. *Inorg. Chem.* **1992**, *31*, 4040.

(19) Atkins, T. J.; Richman, J. E.; Oettle, W. F. *Org. Synth.* **1978**, *58*, 86.

(20) Larson, E. J.; Pecoraro, V. *J. Am. Chem. Soc.* **1991**, *113*, 3810.

(21) Paul, M. A.; Long, F. A. *Chem. Rev.* **1957**, *57*, 1.

(22) (a) Gritzner, G.; Kuta, J. *Pure Appl. Chem.* **1984**, *56*, 461. (b) Geiger, W. E. In *Organometallic Radical Processes*; Troglor, W. C., Ed.; Elsevier: Amsterdam, 1993; p 144. (c) Zaneller, P.; Opromolla, G.; Pardi, L.; Pannell, K. H.; Sharma, H. K. *J. Organomet. Chem.* **1993**, *450*, 193. (d) Bond, A. M.; McLennan, E. A.; Stojanovic, R. S.; Thomas, F. G. *Anal. Chem.* **1987**, *59*, 2853.

(23) Krejčík, M.; Danek, M.; Hartl, F. *J. Electroanal. Chem. Interfacial Electrochem.* **1991**, *317*, 179.

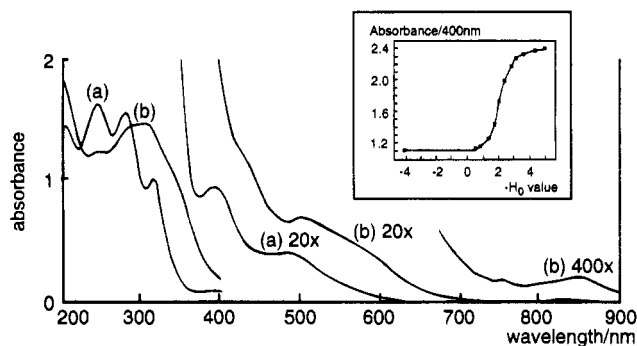


Figure 1. Electronic absorption spectra of $[\text{Mn}^{\text{IV}}_2(\mu\text{-O})_3\text{L}'_2]^{2+}$ in water (a) and in 50% $\text{H}_2\text{SO}_4/\text{H}_2\text{O}$ (v/v) (b). Inset: Plot of the absorbance at 400 nm vs $-H_0$ value (corrected for dilution).

Preparative exhaustive electrolysis of **1** (1 mmol/L) was carried out in citric acid buffer at pH = 9. After reduction of **1**, an excess of aqueous NaBPh_4 solution was added and the precipitate (**3**) was isolated and analyzed. Anal. Calcd for $[\text{Mn}_2(\mu\text{-O})_2(\mu\text{-OH})\text{L}'_2](\text{BPh}_4)_2 \cdot 2\text{H}_2\text{O}$ (**3**): C, 67.14; H, 7.46; N, 7.15; B, 1.83. Found: C, 67.51; H, 7.60; N, 7.10; B, 1.80.

EPR spectra were recorded on a Bruker ECS 106 spectrometer at 77 K.

Results and Discussion

Protonation of $[\text{Mn}^{\text{IV}}_2(\mu\text{-O})_3\text{L}'_2](\text{PF}_6)_2 \cdot \text{H}_2\text{O}$. As shown recently by Wieghardt and co-workers, $[\text{Mn}^{\text{IV}}_2(\mu\text{-O})_3\text{L}'_2](\text{ClO}_4)_2$ can be protonated by adding perchloric acid to a solution containing the dinuclear complex.¹⁴ The X-ray structure of $[\text{Mn}^{\text{IV}}_2(\mu\text{-O})_2(\mu\text{-OH})\text{L}'_2](\text{ClO}_4)_3$ has revealed a longer Mn–Mn distance with a concomitant decrease in the metal–metal interaction.¹⁴ Adding sulfuric acid to an aqueous solution containing 10^{-3} M $[\text{Mn}^{\text{IV}}_2(\mu\text{-O})_3\text{L}'_2](\text{PF}_6)_2 \cdot \text{H}_2\text{O}$ (**1**) results in a significant change in the absorption spectrum (Figure 1). The same absorption spectrum was obtained after addition of concentrated perchloric acid to **1**, showing that no exchange reactions with sulfate had taken place. The absorption spectrum did not change when more concentrated sulfuric acid was added until $-H_0 = 7$, suggesting that the second protonation step is very difficult to achieve. By plotting the absorbance at different wavelengths versus the acidity strength of the solution, we have obtained satisfactory titration plots (Figure 1). The inflection point has been determined to be -2.0 ± 0.1 . Diluting the solution again yielded a nearly quantitative recovery (>95%) of the parent compound, implying that the protonation is reversible and thus that the stability of the protonated complex in acidic solutions is high. No change in the electronic spectrum has been observed between pH = 1 and 13, which suggests that no protonation of the oxygen bridges occurs in this pH range.

The pK_a value of -2.0 found for $[\text{Mn}^{\text{IV}}_2(\mu\text{-O})_3\text{L}'_2]^{2+}$ is much lower than that of $[\text{Mn}^{\text{IV}}_4(\mu\text{-O})_6\text{L}_4]^{4+}$ ($\text{L} = 1,4,7\text{-triazacyclononane}$), which has a pK_a value of 3.5.²⁴ This difference can be accounted for by electronic and steric effects. It has been shown before that the $\text{Mn}^{\text{III}}\text{Mn}^{\text{III}} \rightleftharpoons \text{Mn}^{\text{III}}\text{Mn}^{\text{IV}}$ oxidation potential of $[\text{Mn}_2(\mu\text{-O})(\mu\text{-CH}_3\text{COO})_2\text{L}_2]^{2+}$ is 300 mV lower than that of the analogous L' compound.⁷ The lower oxidation potential suggests a weaker σ -donor character of the L' ligand, which may account for the low pK_a value observed for **1**. Unfortunately, only L' is known to form the $[\text{Mn}^{\text{IV}}_2(\mu\text{-O})_3\text{L}'_2]^{2+}$ structure, which precludes a direct comparison between the pK_a value of the hypothetical 1,4,7-triazacyclononane (L) dimer and **1**.

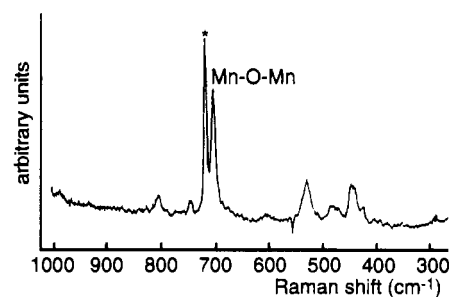


Figure 2. Resonance Raman spectrum of $[\text{Mn}^{\text{IV}}_2(\mu\text{-O})_3\text{L}'_2](\text{PF}_6)_2$ in a KNO_3 pellet, excited by the 457.9 nm laser line.

IR and Resonance Raman Spectra of $[\text{Mn}^{\text{IV}}_2(\mu\text{-O})_3\text{L}'_2]^{2+}$ and $[\text{Mn}^{\text{IV}}_2(\mu\text{-O})_2(\mu\text{-OH})\text{L}'_2]^{3+}$. By using the ^{18}O -labeled complex, the asymmetric Mn–O–Mn vibration in the infrared spectrum and the symmetrical Mn–O–Mn vibration in the resonance Raman (rR) spectrum could be assigned. $[\text{Mn}^{\text{IV}}_2(\mu\text{-}^{16}\text{O})_3\text{L}'_2](\text{PF}_6)_2 \cdot \text{H}_2\text{O}$ (**1**) and the ^{18}O -labeled analog show the asymmetrical Mn–O–Mn vibrations at 670 and 642 cm^{-1} , respectively. The rR spectrum of **1** in a KNO_3 pellet is shown in Figure 2. The symmetrical Mn– ^{16}O –Mn vibration has a frequency of 701 cm^{-1} and that of the corresponding Mn– ^{18}O –Mn vibration is 668 cm^{-1} ($\lambda_{\text{exc}} = 488$ nm). For **1** the symmetrical vibration observed in the rR spectrum is present at a higher frequency than the asymmetrical Mn–O–Mn vibration observed in the IR spectrum. This result contrasts with earlier observations for a series of dinuclear iron complexes.²⁵

The rR spectra ($\lambda_{\text{exc}} = 457.9$ nm) of the protonated complex exhibit symmetrical Mn– ^{16}O –Mn and Mn– ^{18}O –Mn vibrations at 683 and 650 cm^{-1} , respectively. The IR spectrum of this protonated complex exhibits the asymmetrical Mn– ^{16}O –Mn vibration also at 683 cm^{-1} . The shift to lower frequency for the symmetrical Mn–O–Mn vibration (rR) and to higher frequency for the asymmetrical one (IR) upon protonation may be related to a larger Mn–O–Mn angle for the protonated complex (81°)¹⁴ than for **1** (78°).¹² A similar situation applies for $[\text{Mn}^{\text{IV}}_4(\mu\text{-O})_6\text{L}_4](\text{ClO}_4)_4$, since an increase of the Mn–O–Mn angle from $127.4\text{--}128.5^\circ$ to $129.2\text{--}130.9^\circ$ has been observed upon protonation of the complex.¹⁸ The same effect has been observed earlier for a large number of dinuclear, oxo-bridged iron complexes.²⁵ Unfortunately, the number of dinuclear Mn(IV) complexes with good structural data and IR/Raman vibrational data is scarce,^{26,27} and therefore, such a relationship between Mn–O–Mn angles and vibrational frequencies cannot further be elaborated for these complexes.

Electrochemical Behavior in Acetonitrile. A reduction peak has been observed for **1** at -0.98 V vs the ferrocene/ferrocenium redox couple (Fc/Fc^+) with differential pulse voltammetry (DPV) in acetonitrile. Comparison of the peak area with that of a standard single-electron oxidant, $[\text{Ru}(\text{bpy})_3]^{2+}$ (10^{-3} M), suggested the presence of a one-electron cathodic process for **1**. To prove that assignment, we have carried out additional EPR experiments by adding $\text{Co}(\text{Cp})_2$ as a one-electron reductant to an acetonitrile solution containing **1**. $\text{Co}(\text{Cp})_2$ has a reduction potential of -1.39 V vs Fc/Fc^+ and therefore is able to reduce **1** quantitatively. Dissolving 30 mg of $\text{Co}(\text{Cp})_2$ in 15 mL of hot acetonitrile and addition of 100 mg of **1** yield a species that exhibits a 16-line spectrum with a hyperfine coupling constant (a_{Mn}) of approximately 69 G at 77 K (Figure

(25) Sanders-Loehr, J.; Wheeler, W. D.; Shiemke, A. K.; Averill, B. A.; Loehr, T. M. *J. Am. Chem. Soc.* **1989**, *111*, 8084.

(26) Dave, B. C.; Czernuszewicz. *Inorg. Chim. Acta* **1994**, *227*, 33.

(27) Gamelin, D. R.; Kirk, M. L.; Stemmler, T. L.; Pal, S.; Armstrong, W. H.; Penner-Hahn, J. E.; Solomon, E. I. *J. Am. Chem. Soc.* **1994**, *116*, 2392.

(24) Hagen, K. S.; Westmoreland, T. D.; Scott, M. J.; Armstrong, W. H. *J. Am. Chem. Soc.* **1989**, *111*, 1907.

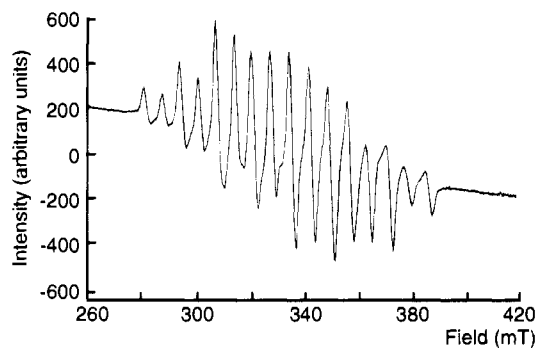


Figure 3. EPR spectrum of **1** reduced by $\text{Co}(\text{Cp})_2$ in acetonitrile at 77 K.

3) due to the presence of two ^{55}Mn nuclei ($I = 5/2$). Although such an EPR spectrum is typical of a mixed-valence $\text{Mn}^{\text{III}}\text{Mn}^{\text{IV}}$ species,^{5e} the hyperfine splitting observed is quite small. Most of the $\text{Mn}^{\text{III}}\text{Mn}^{\text{IV}}$ complexes reported up till now exhibit 16-line spectra with a_{Mn} values of around 77 G.⁵

Interestingly, the reduction wave is found at an unusually low potential.^{5e} Most dinuclear $\text{Mn}^{\text{IV}}\text{Mn}^{\text{IV}}$ complexes characterized so far with two oxygen bridges exhibit reduction potentials between 0.6 and 1.5 V *vs* SCE.^{5e} $[\text{Mn}_2(\mu\text{-O})_2(\text{salpn})_2]$ is the only compound which has a similar reduction potential (-0.39 V *vs* SCE or -0.78 V *vs* ferrocene) ($\text{H}_2\text{salpn} = N,N'$ -bis(salicylidene-1,3-diaminopropane)).²⁸ Undoubtedly, the strong donor properties of the three oxygen bridges cause the decrease of the reduction potential and stabilization of the high-valent $\text{Mn}^{\text{IV}}\text{Mn}^{\text{IV}}$ complex, which is in agreement with the low $\text{p}K_{\text{a}}$ value determined. The factors which influence the redox properties of related dinuclear Mn complexes have been discussed recently.^{5e}

Performing cyclic voltammetry (CV) of **1** with a scan rate of 100 mV s^{-1} , we observe chemically irreversible reduction of **1** at $E_{\text{p,c}} = -1.00$ V *vs* Fc/Fc^+ (Figure 4A). Scanning back from -1.5 to $+0.5$ V *vs* Fc/Fc^+ yields a small anodic peak at $E_{\text{p,a}} = +0.0$ V *vs* Fc/Fc^+ . The latter peak is observed only after passing the reduction of the parent compound **1**. Addition of $\text{Co}(\text{Cp})_2$ to the solution led to the occurrence of a peak at $E_{\text{p,a}} = +0.0$ V *vs* Fc/Fc^+ as well. Thus upon the reduction of **1**, either electrochemically or chemically, a secondary chemical reaction takes place. The product of this reaction is then reoxidized at 0.0 V. No anodic process has been found for **1** up to $+1.5$ V *vs* Fc/Fc^+ , showing that the oxidation $\text{Mn}^{\text{IV}}\text{Mn}^{\text{IV}} \rightarrow \text{Mn}^{\text{V}}\text{Mn}^{\text{IV}}$ should occur at a higher positive potential.

In an acetonitrile solution containing 0.25 M H_2SO_4 and 0.1 M NBu_4ClO_4 , the reduction peak of **1** has been observed with DPV at 0.70 V *vs* Fc/Fc^+ . CV shows an electrochemically quasi-reversible reduction wave at 0.69 V *vs* Fc/Fc^+ with a peak-to-peak separation of 160 mV at 100 mV s^{-1} scan rate (Figure 4b). Accounting for the aforementioned protonation of one oxygen bridge in **1** under these acidic conditions, the CV results imply that protonated **1** is reduced at a considerably higher positive potential in comparison with its nonprotonated form. The positive potential shift of 1.7 V can reasonably be attributed to a drastically decreased donor power of the oxygen bridge upon protonation leading to a more electron-deficient Mn^{IV} center.

Spectroelectrochemistry. By using the OTTLE cell,²³ *in situ* one-electron reduction of 10^{-2} M **1** in acetonitrile was carried out, and the UV-vis and IR spectra of the reduced species were recorded. In the course of the reduction, the solution gradually changed from bright red to brown. The

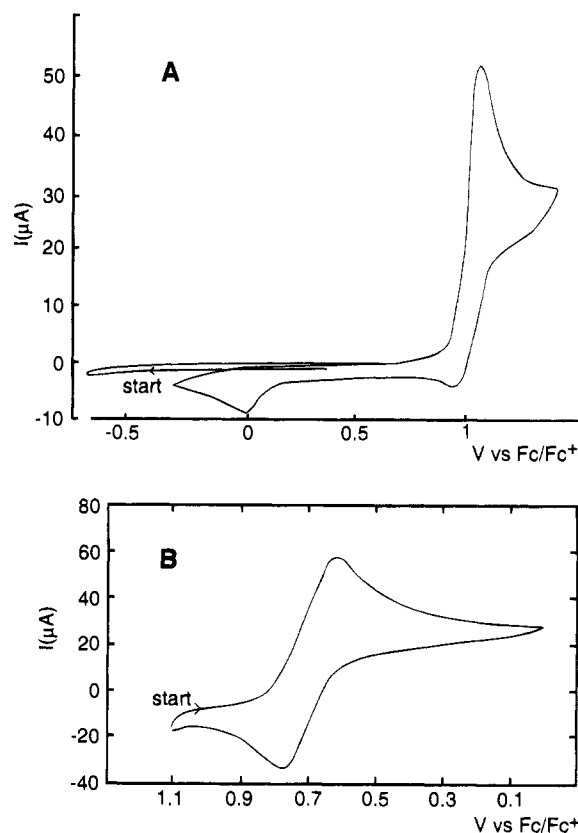


Figure 4. Cyclic voltammograms (100 mV s^{-1}) of $[\text{Mn}^{\text{IV}}_2(\mu\text{-O})_3\text{L}'_2]^{2+}$ in $\text{CH}_3\text{CN}/0.1 \text{ M } [\text{NBu}_4]\text{ClO}_4$ (A) and $[\text{Mn}^{\text{IV}}_2(\mu\text{-O})_2(\mu\text{-OH})\text{L}'_2]^{3+}$ in acetonitrile containing 0.25 M H_2SO_4 and 0.1 M $[\text{NBu}_4]\text{ClO}_4$ (B).

distinct absorption bands of **1** at 390 and 490 nm were replaced by unstructured absorption between 300 and 700 nm. Reoxidation of the species at 0.0 V led to complete recovery of **1**.

The IR absorptions of the parent compound at 791, 990, and 1007 cm^{-1} disappeared, while a new band at 1016 cm^{-1} became visible in the course of the reduction. Interestingly, the vibration at 668 cm^{-1} that has been assigned to $\nu_{\text{as}}(\text{Mn}-^{16}\text{O}-\text{Mn})$ and reflects the $\text{Mn}-\text{O}-\text{Mn}$ angle (*vide supra*) does not change upon reduction of the complex. Also the vibration at 642 cm^{-1} of $[\text{Mn}^{\text{IV}}_2(\mu\text{-}^{18}\text{O})_3\text{L}'_2]^{2+}$ does not shift upon reduction. These observations imply that the $\text{Mn}-\text{O}-\text{Mn}$ angle does not change significantly and consequently that the structure of the reduced species is not altered to a large extent. It is noted that the peaks at 668 and 642 cm^{-1} become only slightly broader and lower in intensity upon complete one-electron reduction of both the ^{16}O - and ^{18}O -labeled compounds, respectively.

On the basis of these results, it is proposed that the reduced species contains either a $\text{Mn}_2(\mu\text{-O})_3$ core or a $\text{Mn}_2(\mu\text{-O})_2(\mu\text{-OH})$ core with similar $\text{Mn}-\text{O}-\text{Mn}$ angles as the parent compound. Formation of dinuclear Mn species containing solely two oxygen bridges would result in a larger $\text{Mn}-\text{O}-\text{Mn}$ angle⁵ and thus in a clear shift of the $\text{Mn}-\text{O}-\text{Mn}$ vibration.

The electrochemical experiments described before have shown that the reoxidation peak of the reduced species of **1** is found at a much higher potential than the reduction peak of **1**. These results and the IR data suggest that, upon reduction of $[\text{Mn}^{\text{IV}}_2(\mu\text{-O})_3\text{L}'_2]^{2+}$, a protonation step may take place, *i.e.* that an EC mechanism operates. Proton donors in acetonitrile, such as water, may cause protonation of the reduced manganese compound. In the presence of sulfuric acid already the dinuclear manganese complex **1** becomes protonated and the electrochemically quasi-reversible reduction is then observed. A

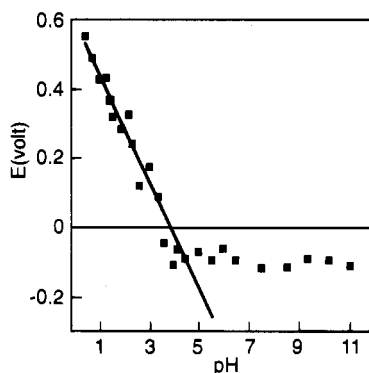
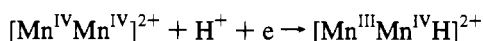


Figure 5. Pourbaix diagram for $[\text{Mn}^{\text{IV}}_2(\mu\text{-O})_3\text{L}'_2]^{2+}$ in 0.2 M citrate buffer.

reduction-induced protonation process is also in agreement with the electrochemical measurements in aqueous solutions (*vide infra*).

pH-Dependent Reduction Processes in Aqueous Solutions.

The reduction process of **1** (0.63 mM) has been studied with DPV in an aqueous citrate buffer (0.2 M) solution at various pH values. The pH dependency of the reduction potentials as deduced from DPV measurements is shown in Figure 5. The reduction potentials vary from +0.54 V at pH = 0.43 to around -0.1 V *vs* SCE between pH = 4 and 10. The observed peak width at half-height ($W_{1/2}$) in the DPV is considerably larger than the theoretical value for a reversible one-electron redox process (90.4 mV).²⁹ Between pH = 7 and 11, the peak width is between 100 and 120 mV, whereas below pH = 7, the peak width increases up to 360 mV (pH = 3.6) and decreases again at lower pH values (120 mV at pH = 0.47). The broadness of the DPV peaks at nearly all pH values is indicative of an irreversible reduction process, as confirmed by CV measurements (irreversible reduction; *vide supra*). Activation of the glassy-carbon electrode as described by Meyer³⁰ and Brudwig¹⁶ *et al.* did not bring any improvement. The shift of the reduction potential to higher values upon lowering the pH suggests that below pH = 4 the electrochemical reduction is coupled with a proton-transfer process:



As shown in Figure 5, the slope of the $E_{1/2}$ -pH plot (Pourbaix diagram) is about 155(11) mV/pH unit, which is significantly higher than the theoretical value for a coupled $1\text{H}^+/1e^-$ process in a reversible redox reaction (59 mV/pH).¹⁶ Two possible explanations can account for this behavior. Disproportionation reactions between the reduced species occur, as observed in a number of other cases.^{12,28} This may be reflected in a [1] dependence of the slope of the Pourbaix diagram. However, changing the concentration of complex does not lead to a change in the slope.³¹ A plausible explanation for the steep slope of the reduction potential *vs* pH dependence may be that in this case the reduction is clearly irreversible, leading to significant deviations from the "ideal" Nernst shift per pH unit for a coupled $1\text{H}^+/1e^-$ process (59 mV/pH).¹⁶ Extrapolation of the experimental slope of 144 mV/pH unit observed to a pH -2.0 implies a reduction potential of 0.90 V *vs* SCE at this pH. This agrees quite well with the observed value of 0.87 V *vs* SCE (0.76 V *vs* Fc/Fc^+) for the protonated complex in acetonitrile/ H_2SO_4

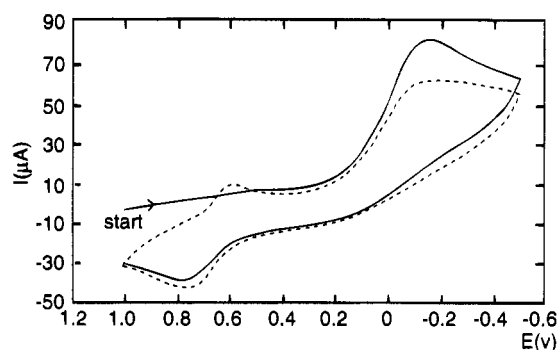


Figure 6. Cyclic voltammograms of $[\text{Mn}^{\text{IV}}_2(\mu\text{-O})_3\text{L}'_2]^{2+}$ in citrate buffer at pH = 3.61 (100 mV s⁻¹). (—) first scan; (---) second scan.

solution. pH-dependent electrochemical experiments in phosphate and Me_3TACN yield similar results.³²

In solutions having pH > 4, no coupled electron-proton transfer process takes place. The pH-independent region at pH > 4 for $[\text{Mn}^{\text{IV}}_2(\mu\text{-O})_3\text{L}'_2]^{2+}$ suggests that the $\text{p}K_a$ for the $\text{Mn}^{\text{III}}\text{-Mn}^{\text{IV}}$ species is about 4. Care should be taken in using these data, as the reduction process is electrochemically or chemically irreversible (*vide supra*), which may lead to deviations of the $\text{p}K_a$ value. It is clear, however, that the $\text{p}K_a$ of the reduced species is much higher than that of **1**. A large increase in the $\text{p}K_a$ value in passing from the $\text{Mn}^{\text{IV}}\text{Mn}^{\text{III}}$ to a $\text{Mn}^{\text{III}}\text{Mn}^{\text{III}}$ state has been observed for $[\text{Mn}_2(\mu\text{-O})_2(\text{bpy})_4]^{2+}$ as well (from 2.3 to 11.0).¹⁶ These results can again be explained by less electron donation from oxygen to manganese for the manganese ion in a lower oxidation state.

Electrochemically-Induced Formation of Other Species.

The DPV's in the presence of citrate buffer suggest an irreversible reduction of **1** (*vide supra*). This has been confirmed by carrying out cyclic voltammetry. As shown in Figure 6, a chemically irreversible wave at 0.02 V at pH = 3.61 in 0.2 M citrate buffer was observed. Upon scanning back from -0.5 to +1.0 V, we observed a new anodic peak at 0.68 V with the corresponding cathodic counterpeak at 0.57 V. This implies that the reduction of **1** is followed by a secondary reaction of the primary $\text{Mn}^{\text{III}}\text{Mn}^{\text{IV}}$ product, giving a relatively stable compound. This wave was only observed at $[\text{citrate}] > 10^{-3}$ M. In other buffer systems containing carboxylate groups, such as succinic acid and acetic acid, the redox couple occurs between 0.5 and 0.8 V as well, although in the latter buffer the wave is much more difficult to discern. No voltammetric peaks between 0.5 and 0.8 V were observed upon using L' as the buffer system. Bulk electrolysis experiments were carried out to obtain information on the nature of the species formed. Applying a potential of -0.4 V *vs* SCE to a solution of **1** in a 0.2 M citrate buffer at pH = 3.5 caused the color of the solution to change from bright red to brownish-purple. The UV-vis spectrum of the electrolyzed solution exhibited two bands at 485 and 515 nm and a weak band at 725 nm. Such an absorption spectrum is very typical of a $[\text{Mn}^{\text{III}}_2(\mu\text{-O})(\mu\text{-XCOO})_2\text{L}_2]^{2+}$ species.¹² Addition of $[\text{Mn}^{\text{III}}_2(\mu\text{-O})(\mu\text{-H}_3\text{CCOO})_2\text{L}'_2]^{2+}$ (**2**) to a 0.5 M citrate solution leads to a slow decrease of $E_{p,a}/E_{p,c}$ at 0.80/0.71 V (originating from **2**) and a concomitant increase of the redox couple at 0.68/0.57 V as judged from CV measurements.

(29) Bard, A. J.; Faulkner, L. R. *Electrochemical Methods, Fundamentals and Applications*; John Wiley and Sons: New York, 1980.

(30) Roecker, L.; Kutner, W.; Gilbert, J. A.; Simmons, M.; Murray, R. W.; Meyer, T. J. *Inorg. Chem.* **1985**, *24*, 3784.

(31) Using 1.26 mM instead of 0.63 mM complex leads to a similar Pourbaix diagram with a slope of 145(4) mV/pH unit.

(32) Using 0.2 M phosphate as buffer yields a slope of 159(10) mV/pH unit, an apparent $\text{p}K_a$ value for the $\text{Mn}^{\text{III}}\text{Mn}^{\text{IV}}$ species of 4.5, and a calculated reduction potential of 0.94 V at pH -2.0. Using 0.2 M L' as buffer yields a slope of 169(10) mV/pH, a $\text{p}K_a$ value of 4.0, and a calculated reduction potential of 0.77 V at pH -2.0. The ligand as buffer was chosen because the use of a free ligand may improve the reversibility of the cyclic voltammograms considerably.¹⁵

These results strongly suggest that, upon electrochemical reduction of **1** in citrate buffer, a dinuclear Mn^{III} species with two carboxylate bridges is formed. Addition of 1 equiv of ascorbic acid as reductant to **1** at this pH in the presence of citrate or acetate buffer leads to the formation of a species having a similar UV-vis spectrum as well.³³ Reduction of **1** at pH 1 with ascorbic acid leads to a gradual decrease of bands at 490 and 390 nm and a concomitant formation of a six-line EPR spectrum ($a_{\text{Mn}} = 88$ G), showing that under these conditions mainly Mn(II) species are formed. This can be explained by disproportionation reactions at low pH due to protonation of the oxygen bridges.^{34,35}

Exhaustive electrolysis of **1** at -0.8 V vs SCE in citrate buffer of pH 9 yielded, after addition of a NaBPh₄ solution, a yellow-brown precipitate (**3**) that was further analyzed. The EPR spectrum of **3** exhibits a 16-line signal with the same hyperfine constant (a_{Mn}) as that described above for the product of the chemical reduction of **1** in acetonitrile (Figure 3).³⁶ Furthermore, the Mn-O-Mn vibration (IR) and the UV-vis spectrum (dmf) of compound **3** are very similar to those obtained by the *in situ* OTTLE reduction of **1** (*vide supra*). The IR spectrum of **3** shows also a broad band at around 3600 cm^{-1} , characteristic of the presence of OH groups. These results suggest that species **3** is the same species observed upon reduction of **1** in acetonitrile and contains the Mn^{III}(μ -OH)(μ -O)₂Mn^{IV} core.

Concluding Remarks

We have shown that $[\text{Mn}_2(\mu\text{-O})_3\text{L}'_2]^{2+}$ exhibits interesting electrochemical properties. The pH-dependent electrochemical studies have revealed that the potential of the reduction peak gradually shifts to higher values when the pH is lowered. The slope of the Pourbaix diagram is much steeper than the theoretical value for reversible systems. Varying the buffer systems and complex concentration has revealed that the slope of the Pourbaix diagram is not influenced significantly. The irreversible nature of the reduction process may have caused this discrepancy in the pH-dependent behavior. The UV-vis, EPR, and IR data have suggested the presence of a Mn₂(μ -O)₂(μ -OH) core upon reduction of **1** in CH₃CN. Electrochemical reduction of **1** in aqueous solution at pH 9 afforded, after addition of NaBPh₄, a precipitate that exhibits similar spectra, suggesting that identical species are formed upon reduction in acetonitrile and water. Measurements in citrate buffers of citrate concentrations > 1 mM have shown that, upon one-electron reduction, disproportionation reactions yield a bis(carboxylato)-bridged species. A major difference between $[\text{Mn}_2(\mu\text{-O})_3\text{L}'_2]^{2+}$ and the dinuclear Mn(μ -O)₂ compounds studied up till now is the much lower pH window in which the H⁺/e processes are observed. This is undoubtedly caused by the unique structure of this molecule with three donating oxygen atoms bridging the Mn^{IV} ions.

Acknowledgment. We thank Prof. Karl Wieghardt for useful discussions. The authors are indebted to Mr. A. M. van Loon for additional experiments.

IC941205+

- (33) Subsequent addition of aqueous sodium tetraphenylborate to the solutions containing **1**, ascorbic acid, and citrate or acetate buffer yields purple precipitates. IR of the acetate compound has the same vibrations as the genuine material (COO vibrations at 1572 , 1460 , and 1424 cm^{-1}).⁷ The UV-vis spectrum (CH₃CN) of this complex exhibits bands at 720 , 520 , 485 , and 310 nm , in agreement with the literature values.^{8,12} The compound isolated in citrate buffer contains strong IR absorptions at 1590 , 1464 , and 1426 cm^{-1} . The UV-vis spectrum of this compound in acetonitrile shows bands at 720 , 520 , 485 , and 310 nm , the same bands as found for the acetate analog and the sample obtained by coulometry.
- (34) Sarneski, J. E.; Thorp, H. H.; Brudwig, G. W.; Crabtree, R. H.; Schulte, G. K. *J. Am. Chem. Soc.* **1990**, *112*, 7255.
- (35) Philouze, C.; Blondin, G.; Girerd, J.-J.; Guilheim, J.; Pascard, C.; Lexa, D. *J. Am. Chem. Soc.* **1994**, *116*, 8557.

- (36) It is noted that this EPR spectrum is different from the one discussed recently.³⁷ The EPR spectrum discussed in this paper has a hyperfine constant of 69 G , while the 16-line spectrum reported elsewhere³⁷ has a hyperfine constant of 77 G . The hyperfine splitting of 77 G is very typical for mixed-valence Mn^{III}Mn^{IV} species, as discussed elsewhere.⁵
- (37) Hage, R.; Iburg, J. E.; Kerschner, J.; Koek, J. H.; Lempers, E. L. M.; Martens, R. J.; Racherla, U.; Russell, S. W.; Swarthoff, T.; van Vliet, M. R. P.; Warnaar, J. B.; van der Wolf, L.; Krijnen, B. *Nature* **1994**, *369*, 637.